

Quantum degeneracy and interaction effects in spin-polarized Fermi-Bose mixtures

L. Vichi^a, M. Inguscio^b, S. Stringari^a, G. M. Tino^c

^a *Dipartimento di Fisica, Università di Trento and Istituto Nazionale per la Fisica della Materia, I-38050 Povo, Italy*

^b *Dipartimento di Fisica and European Laboratory for Nonlinear Spectroscopy (LENs), Università di Firenze, and Istituto Nazionale per la Fisica della Materia, Largo E. Fermi 2, I-50125 Firenze, Italy*

^c *Dipartimento di Scienze Fisiche, Università di Napoli “Federico II” and Istituto Nazionale per la Fisica della Materia, Complesso Universitario di Monte S. Angelo, via Cintia, I-80126 Napoli, Italy*

(November 5, 2021)

Various features of spin-polarized Fermi gases confined in harmonic traps are discussed, taking into account possible perspectives of experimental measurements. The mechanism of the expansion of the gas is explicitly investigated and compared with the one of an interacting Bose gas. The role of interactions on the equilibrium and non equilibrium behaviour of the fermionic component in Fermi-Bose mixtures is discussed. Special emphasis is given to the case of potassium isotopes mixtures.

I. INTRODUCTION

After the achievement of Bose-Einstein condensation (BEC) in dilute vapors of alkali atoms confined in magnetic traps [1–3], a challenge for future experiments is the cooling of samples of fermionic atoms, down to the degenerate regime.

This perspective has already motivated several theoretical works (see, for example, [4,5]) devoted to the study of a possible superfluid phase occurring at very low temperature, analog to the one exhibited by superfluid ³He and superconductors. The behaviour of this transition depends crucially on the sign and the size of the scattering length and various predictions have already been made to estimate the value of the corresponding critical temperature. Another peculiar phenomenon exhibited by finite Fermi gases at low temperature is the occurrence of quantum shell effects [6], bringing interesting analogies with the physics of atomic nuclei and metal clusters. The observation of such phenomena is seriously limited by the difficulty of reaching the required regime of very low temperatures. In fact both superfluidity and shell effects are expected to occur at temperatures much smaller than the Fermi temperature. For a realistic perspective of experimental measurements in the immediate future it is consequently useful to explore quantum degeneracy effects taking place at higher temperature. These effects have been already the subject of several theoretical works [7–10,6,11–14].

A crucial role in the experimental achievement of the low temperature regime needed to observe quantum degeneracy effects is played by evaporative cooling. This technique requires frequent collisions in order to ensure fast thermalization. Scattering between spin-polarized fermions in *s* wave is inhibited by the Pauli exclusion principle. As a consequence one should look for alternative scattering processes involving different spin states or atoms belonging to different species. Fermi-Bose or Fermi-Fermi mixtures are possible candidates. The resulting scattering processes will eventually provide the relevant thermalization mechanism, allowing for the cool-

ing of the sample (sympathetic cooling [15,16]).

In the following we will mainly discuss the case of Fermi-Bose mixtures where the effects of two-body interactions can be significant also on the equilibrium properties of the fermionic component because of the occurrence of Bose-Einstein condensation which strongly enhances the value of the central density below the critical temperature, thereby emphasizing the effects of the mean field interaction. In this context we will limit the discussion to the case of spin-polarized Fermi gases where the interaction between fermions can be safely neglected. Notice that in the case of unpolarized Fermi gases also the interaction between fermions can produce significant effects on the equilibrium properties if the scattering length is large as happens, for example, in the case of ⁶Li [4,13].

The aim of the present paper is to discuss some of the key features exhibited by spin-polarized trapped Fermi gases, with special emphasis to the dynamics of the expansion following the switching off of the trap (Sect. II) and the role of interactions in the case of Fermi-Bose mixtures (Sect. III). We apply the results to the case of ⁴⁰K, the fermionic isotope of potassium, which has been recently cooled in a magneto-optical trap [17]. Potassium is in fact a good candidate for the experiments proposed here because of the presence of two bosonic isotopes, ³⁹K and ⁴¹K in addition to the fermionic one. The possibility of magnetically trapping these atoms has been already demonstrated [18]. Collisional cross sections for potassium have been calculated in [19,20]. In the following we assume the values given in [20]. The analysis presented in the present paper can be easily extended to other fermionic atoms which are presently investigated experimentally as, for instance, ⁶Li [21].

II. THE IDEAL FERMION GAS

The thermodynamic behaviour of ideal trapped Fermi gas has already been investigated [8–10,6]. In this section we summarize the main results and we derive explicit formulae for the expansion of the fermionic cloud after

turning off the confining potential. These results could be relevant in view of future measurements on the expanding cloud.

Let us consider N fermions trapped in an axially symmetric harmonic potential

$$V(r_\perp, z) = \frac{1}{2}m(\omega_\perp^2 r_\perp^2 + \omega_z^2 z^2) \quad (1)$$

and ignore the effects of the two-body interatomic force. The particle distribution function can be written, in semiclassical approximation, as

$$n(\mathbf{r}, \mathbf{k}, \beta) = \frac{1}{(2\pi)^3} \frac{1}{\exp(\beta(\frac{\hbar^2 k^2}{2m} + V(r_\perp, z) - \mu_f)) + 1}, \quad (2)$$

where $\beta = (K_B T)^{-1}$ and μ_f is the chemical potential, fixed by the normalization condition

$$N = \int n(\mathbf{r}, \mathbf{k}, \beta) d\mathbf{r} d\mathbf{k} = \frac{1}{2(\hbar\omega)^3} \int_0^\infty \frac{E^2 dE}{e^{\beta(E-\mu_f)} + 1}. \quad (3)$$

In eq. (3) $\omega = (\omega_\perp^2 \omega_z)^{1/3}$ is the geometrical average of the trapping frequencies.

If more spin states are occupied, then (2) characterizes the distribution function of each component separately. It can differ from a component to another because the number of atoms in each spin state and the corresponding trapping potential are in general different.

At $T = 0$ eq. (3) allows one to calculate the Fermi energy defined by $E_F = \mu_f(T = 0)$. One finds

$$E_F = K_B T_F = (6N)^{1/3} \hbar\omega. \quad (4)$$

The Fermi energy (4) can be used to define typical length and momentum scales [10] characterizing the Fermi distribution in coordinate and momentum space respectively:

$$E_F = \frac{1}{2}m\omega_\perp^2 R_\perp^2 = \frac{1}{2}m\omega_z^2 Z^2 = \frac{\hbar^2 K_F^2}{2m} \quad (5)$$

where R_\perp and Z are the radial and axial widths of the density distribution at zero temperature:

$$n(\mathbf{r}; T = 0) = \frac{8}{\pi^2} \frac{N}{R_\perp^2 Z} \left(1 - \left(\frac{r_\perp}{R_\perp} \right)^2 - \left(\frac{z}{Z} \right)^2 \right)^{3/2} \quad (6)$$

while K_F is the width of the corresponding momentum distribution

$$n(\mathbf{k}; T = 0) = \frac{8}{\pi^2} \frac{N}{K_F^3} \left(1 - \frac{k^2}{K_F^2} \right)^{3/2}. \quad (7)$$

Eqs. (6) and (7) hold for positive values of their arguments. Eq. (7) is the analog of the most familiar momentum distribution $n(k; T = 0) = 3N/(4\pi K_F^3) \Theta(1 - k^2/K_F^2)$ characterizing uniform Fermi gases.

At finite temperature the total energy E of the system can be written in the form

$$E = \frac{1}{2(\hbar\omega)^3} \int_0^\infty \frac{E^3 dE}{e^{\beta(E-\mu_f)} + 1}, \quad (8)$$

while the release energy, given by the energy of the system after switching off the trap is equal to $E_{rel} = E/2$, because of the equipartition theorem. At low temperatures one has $E \simeq \frac{3}{4} N E_F \left(1 + \frac{2\pi}{3} \left(\frac{T}{T_F} \right)^2 \right)$. In Fig. 1 we show the release energy vs T for a gas of N fermions confined in a harmonic trap (solid line). In the same figure we also report the behaviour predicted by the classical gas ($E_{rel} = 3/2 N K_B T$, dashed line) as well as the one of an ideal Bose gas with the same number of particles N , in the same confining trap (dot dashed line). For the ideal Bose gas the release energy is given by $E_{rel} = 1.35 N (K_B T)^4$ for $T < T_c$ where $T_c = 0.94 \hbar\omega N^{1/3}/K_B$ is the critical temperature for Bose-Einstein condensation. Notice that, differently from the Fermi case, Bose gases exhibit a phase transition at $T = T_c$. This temperature has the same N dependence as the Fermi temperature (see eq. (4)) and is fixed by the same geometrical average of the trapping frequency. The general relation between the two temperatures is given by

$$T_F = 1.9 T_c \left(\frac{N_f}{N_b} \right)^{1/3} \frac{\omega_f}{\omega_b} \quad (9)$$

where the suffix f (b) refers to fermions (bosons). The figure clearly shows that in order to observe effects of degeneracy in the release energy of a Fermi gas one should go to temperatures considerably smaller than the Fermi temperature. For example in order to obtain a deviation of 20 percent from the classical value one should work at $T \sim 0.3 T_F$. This represents a major difference with respect to the thermodynamic behavior of a Bose gas where the effects of Bose-Einstein condensation in the release energy show up immediately below the critical temperature as clearly shown in the same figure.

Let us now consider the expansion of the cloud after turning off the trapping potential. To obtain the temporal evolution of the density profile one has to solve the Boltzmann transport equation. For cold and dilute Fermi gases one can ignore two body collisions and the distribution function after switching off the trap will consequently follow the ballistic law $n(\mathbf{r}, \mathbf{k}, \beta, t) \equiv n_0(\mathbf{r} - \frac{\hbar\mathbf{k}}{m}t, \mathbf{k}, \beta)$, where n_0 is the distribution function at $t = 0$, given by (2). One can then easily calculate the time evolution of the spatial density during the expansion for which we find the simple analytic result

$$n(\mathbf{r}, \beta, t) = \frac{6N_f}{R_\perp^2 Z} \frac{1}{(\pi E_F \beta)^{3/2}} \frac{1}{(1 + \omega_\perp^2 t^2)(1 + \omega_z^2 t^2)^{1/2}} f_{3/2}(\tilde{z}) \quad (10)$$

where $f_n(z) = (\Gamma(n))^{-1} \int dy y^{n-1}/(z^{-1}e^y + 1)$ are the Fermi functions, $\tilde{z} = \exp(\beta(\mu_f - \tilde{V}(\mathbf{r}, t)))$ and

$$\tilde{V}(\mathbf{r}, t) = \frac{1}{2}m \left(\frac{\omega_{\perp}^2 r_{\perp}^2}{1 + \omega_{\perp}^2 t^2} + \frac{\omega_z^2 z^2}{1 + \omega_z^2 t^2} \right)$$

plays the role of an effective potential fixing, at each instant, the shape of the distribution function. The chemical potential has no time dependence, being fixed by the normalization condition (3).

From (10) one can extract the temporal evolution of the mean square radii of the system:

$$\langle r_{\perp}^2 \rangle = \frac{1}{3N} E_{rel} \frac{2}{m\omega_{\perp}^2} (1 + \omega_{\perp}^2 t^2) \quad (11)$$

$$\langle z^2 \rangle = \frac{1}{3N} E_{rel} \frac{2}{m\omega_z^2} (1 + \omega_z^2 t^2). \quad (12)$$

which have been written in terms of the release energy $E_{rel} = E/2$ of the gas. The structure of these equations is independent of the temperature which enters the problem only through the value of the release energy, fixing the initial value of the widths. Actually the release energy fixes also the asymptotic behavior of the widths, as clearly shown by eqs. (11-12). In Fig. 2 we compare the temporal evolution, at $T = 0$, of the root mean square radii of the Fermi gas (see eq. 11-12) with the one of a gas of interacting bosons. The Fermi gas corresponds to 10^6 ^{40}K atoms initially confined by a harmonic trap with $\omega_f = 100$ Hz. The Bose gas instead corresponds to 10^6 ^{39}K atoms interacting with a scattering length $a_{bb} = 80 a_0$ [20] (a_0 is the Bohr radius) and initially confined by a magnetic trap with $\omega_b = 100$ Hz. The same parameters have been used to calculate the release energy of the interacting Bose gas as a function of temperature (dotted curve in Fig. 1) in the framework of the theory developed in [22]. Fig. 2 clearly shows that the Fermi gas expands more quickly than the Bose gas due to the significantly higher value of the release energy.

Another useful quantity is the aspect ratio of the cloud

$$R_r(t) = \sqrt{\frac{\langle z^2 \rangle}{\langle x^2 \rangle}} = \frac{1}{\lambda} \sqrt{\frac{1 + \omega_z^2 t^2}{1 + \omega_{\perp}^2 t^2}}. \quad (13)$$

Eq. (13) shows that for $t \rightarrow \infty$ the cloud becomes spherical in shape even if it was initially strongly anisotropic. This behaviour is independent of the temperature and is due to the absence of collisions during the expansion. Notice that in a Bose gas the situation is quite different, the asymptotic distribution being anisotropic due to the occurrence of Bose-Einstein condensation, as explicitly pointed out in the first experiments on BEC [1,2].

III. FERMION-BOSE MIXTURES

It is important to discuss how the scenario presented in the preceding section for the ideal Fermi gas is modified when the system interacts with a Bose gas confined in

the same trap. As discussed in the introduction such mixed Fermi-Bose gases might become relevant in future experiments for the achievement of very low temperature regimes via sympathetic cooling.

The study of Fermi-Bose mixtures has been already the subject of theoretical studies at zero [11] as well as finite temperature [12]. Due to the occurrence of Bose-Einstein condensation the bosonic component is characterized by a high density in the central region of the trap where consequently interaction effects play an important role. The presence of the much more dilute Fermi component is not expected to influence the bosonic wave function in a significant way, so that the main effect of interactions between fermions and bosons will result in an additional external field acting on the Fermi component. The Fermi gas can then, in first approximation, be treated again as an ideal gas trapped by the effective potential

$$V_{eff} = V + g_{bf} n_b(r, T) \quad (14)$$

where V is the external potential (1) trapping the fermionic species, and the renormalization arises from the interaction with bosons. The parameter $g_{bf} = 2\pi\hbar^2 a_{bf}/m_r$ is the Fermi-Bose interaction coupling constant fixed by the relative scattering length a_{bf} and by the reduced mass $m_r = m_b m_f / (m_b + m_f)$. The bosonic density n_b can be calculated at thermal equilibrium using standard procedures developed to describe Bose condensed gases at finite temperature (see for example [22]).

The new equilibrium properties of the Fermi gas can be simply understood by looking at the shape of the potential (14) as explicitly discussed in [12]. A first important feature is that the interaction term in (14) produces a weaker confinement. This results in an expansion of the Fermi cloud with respect to the non interacting case and a consequent decrease of the average density, as well as of quantum statistical effects. The effects are more pronounced at low temperature where all the bosons are in the condensate and one can use the Thomas-Fermi approximation to calculate the density distribution of the bosonic component. In this case one has $n_b = 15N_b(R_b^2 - r^2)/(8\pi R_b^5)$ where $R_b = a_{ho}(15N_b a_{bb}/a_{ho})^{1/5}$ is the classical radius of the Bose gas, a_{bb} is the boson-boson scattering length and $a_{ho} = (\hbar/m_b \omega_b)^{1/2}$ is the oscillator length relative to the bosons. One finds that the effective potential felt by the fermions is given, for $r < R_b$ by [12]

$$V_{eff} = \frac{m_f}{2} \omega_f^2 \left(1 - \frac{g_{bf}}{g_{bb}} \frac{m_b \omega_b^2}{m_f \omega_f^2} \right) r^2 + \frac{g_{bf}}{g_{bb}} \mu_b \quad (15)$$

where, for simplicity, we have considered an isotropic trap. For $r > R_b$ the effective potential instead coincides with the bare potential V . Eq. (15) shows that the oscillator constant is reduced by the interaction with bosons.

As a first example we consider 10^4 ^{40}K atoms and 10^6 ^{39}K atoms confined in the same harmonic trap ($\omega_f =$

ω_b). This corresponds to a realistic case considering the present status of the experiments [17,18]. For the interactions we make the assumption $g_{bf} \sim 0.5g_{bb}$ [20].

The effect of the interactions is to push the fermionic cloud “outside” and to reduce the value of the central density. With the above choice of parameters we find, at $T = 0$, that the central density is reduced by ~ 35 percent, and the average square radius $\langle r^2 \rangle$ increases from $9.5 a_{ho}^2$ to $11.5 a_{ho}^2$. The importance of the interactions on the equilibrium properties of the Fermi component of the mixture is expected to depend in a crucial way on the temperature as well as on the relative concentrations of the two atomic species. For example at $T = T_F$ one finds a much smaller effect due to the interactions. In this case the average square radius increases only by 2.5 %, even if the central density is reduced by 25 %. Notice that in the configuration here considered the Fermi temperature is lower than the critical temperature for BEC: $T_F = 0.4 T_c$. This shows that the effects of quantum degeneracy of the interactions can be observed only at very low temperatures.

Concerning the role of the relative concentrations we point out that from an experimental point of view one can access quite a large range of concentrations. Indeed in [17] 10^4 fermionic potassium atoms were magneto-optical trapped from a natural abundance sample. Since samples enriched by two orders of magnitude are available, 10^6 ^{40}K potassium atoms could be easily loaded. More recently more than 10^8 bosonic isotopes have been trapped in a double MOT apparatus [18] in the ultra high vacuum environmental condition required for evaporative cooling. This method can be easily extended to ^{40}K . Hence Bose-Fermi mixtures are expected to be available in the near future with a large variety of relative abundances. As a second example we have considered the case $N_f = N_b = 10^6$. With these values the Fermi temperature is larger than the BEC temperature ($T_F = 1.9 T_c$). However the effect of the interactions are significantly reduced even at $T = 0$. For example the central density has decreased only by 10 % with respect to the non interacting case.

The above discussion suggests that the main features of the ideal Fermi gas discussed in section II are modified only in a semi quantitative way by the inclusion of the interactions with the bosons. Nevertheless the effects of the interaction could be observed experimentally by removing the bosonic component from the trap at the end of the sympathetic cooling. This can be realized by optical or rf transitions, and corresponds to a sudden switching off of the interaction term at $t = 0$ in the confining potential (15). The result is an undamped oscillation of the Fermi cloud, shown in Fig. 3, according to the law

$$\langle r^2 \rangle(t) = \langle r^2 \rangle_0 + \delta \cos(2\omega_f t), \quad (16)$$

where $\langle r^2 \rangle_0$ is the equilibrium mean radius of the fermions in the trap in absence of interactions, δ is the difference between the value of $\langle r^2 \rangle$ calculated at $t = 0$ and

$\langle r^2 \rangle_0$. This oscillation, which is a direct consequence of the Fermi-Bose interactions, could be observed by imaging the atomic cloud during the expansion.

Another consequence of the interaction between the two components is the occurrence of a shift in the frequency of the relative motion of the Fermi-Bose clouds, with respect to the predictions of the non interacting model. This can be easily calculated in the limit where the number of fermions is much smaller than the one of bosons. In this case the motion of the fermions is described by the potential (15) and the center of mass of the fermionic cloud oscillates with frequency $\omega = \omega_f \left(1 - \frac{g_{bf}}{g_{bb}} \frac{m_b \omega_b^2}{m_f \omega_f^2}\right)^{1/2}$. With the choice of parameters employed above ($\omega_f \sim \omega_b$, $m_b \sim m_f$ and $g_{bf} \sim 0.5g_{bb}$) the frequency is reduced by about 30 percent.

In conclusion we have shown that the behaviour of a spin-polarized degenerate Fermi gas, confined in harmonic traps, exhibits several interesting features, even in the absence of superfluidity. These features, which are the consequence of Fermi pressure effects, are directly observable by looking at the expansion of the gas and are also sensitive to the interactions between fermions and bosons in atomic mixtures.

We would like to thank E. Cornell for useful discussions. This work was supported by the BEC advanced research project of INFM.

-
- [1] M. H. Anderson, J. R. Ensher, M. R. Matthews, C. E. Wieman and E. A. Cornell, Science **269** 198 (1995)
 - [2] K. B. Davis, M. O. Mewes, M. R. Andrews, N. J. van Druten, D. S. Durfee, D. M. Kurn and W. Ketterle, Phys. Rev. Lett. **75**, 3969 (1995)
 - [3] C. C. Bradley, C. A. Sackett and R. G. Hulet, Phys. Rev. Lett **78**, 985 (1997)
 - [4] H. T. C. Stoof *et al.*, Phys. Rev. Lett **76**, 10 (1996)
 - [5] M. Houbiers *et al.*, Phys. Rev. A **56**, 4864 (1997)
 - [6] J. Schneider and H. Wallis, Phys. Rev. A **57** 1253 (1997)
 - [7] E. Fermi, Rend. Lincei, **3**, 145 (1926); Z. Phys. **36**, 902 (1926)
 - [8] Isaac F. Silvera, Physica **109** & **110B** 1499-1522 (1982)
 - [9] J. Oliva, Phys. Rev. B **39** 4204-4209 (1989)
 - [10] D. A. Butts, D. S. Rokhsar, Phys. Rev. A **55** 4346 (1997)
 - [11] K. Molmer, Phys. Rev. Lett. **80** 1804 (1998)
 - [12] M. Amoroso, A. Minguzzi, S. Stringari, M. P. Tosi and L. Vichi, Eur. Phys. Jour. D, in press
 - [13] G. M. Bruun and K. Burnett, preprint physics 9807027
 - [14] B. DeMarco and D. S. Jin, preprint cond-mat 9807406
 - [15] C. J. Myatt, E. A. Burt, R. W. Ghrist, E. A. Cornell and C. E. Wieman, Phys. Rev. Lett., **78**, 586 (1997)
 - [16] E. Timmermans and R. Cote, Phys. Rev. Lett. **80**, 3419 (1998)
 - [17] F. S. Cataliotti, E. A. Cornell, C. Fort, M. Inguscio, F. Marin, M. Prevedelli, L. Ricci and G. M. Tino, Phys.

Rev. A **57**, 1136 (1998)

- [18] M. Prevedelli, F. S. Cataliotti, E. A. Cornell, J. R. Ensher, C. Fort, L. Ricci, G. M. Tino, M. Inguscio, Phys. Rev. A, in press
- [19] H. M. J. M. Boesten, J. M. Vogels, J. G. C. Templaars, B. J. Verhaar, Phys. Rev. A **54** R3726 (1996)
- [20] R. Cote, A. Dalgarno, H. Wang, W. C. Stwalley, Phys. Rev. A, **57**, 4118R (1998)
- [21] E. R. I. Abraham, W. I. McAlexander, J. M. Gerton, R. G. Hulet, R. Cote and A. Dalgarno, Phys. Rev. A **53**, R3713 (1996)
- [22] S. Giorgini, L. P. Pitaevskii and S. Stringari, Jour. Low Temp. Phys. **109** 309 (1997); A. Minguzzi, S. Conti and M. P. Tosi, J. Phys. : Condens. Matter **9**, L33 (1997)

FIGURE CAPTIONS

Fig. 1 Release energy in units of $NK_B T_F$ as a function of temperature (in units of the Fermi temperature T_F). The solid line corresponds to an ideal Fermi gas trapped in a harmonic potential. The dashed line is the linear law of a classical gas, while the dot dashed and the dotted lines are the release energy for a Bose gas with the same number of atoms confined in the same trap in the non-interacting and in the interacting case respectively (see the text).

Fig. 2 Temporal evolution in *msec* of the root mean square radii (in units of a_{ho}) of an ideal Fermi gas of ^{40}K (solid line) and of an interacting Bose gas ^{39}K (dashed line) at zero temperature after switching off the trap. The two curves refer to a trap with $\omega = 100 \text{ Hz}$ and same number of particles $N = 10^6$. The scattering lenght for the ^{39}K was taken from [20].

Fig. 3 Oscillations at zero temperature of the mean square radius of 10^4 ^{40}K atoms after the bosons (10^6 ^{39}K atoms) are removed. Time and lengths are in units of ω/π and a_{ho} respectively.

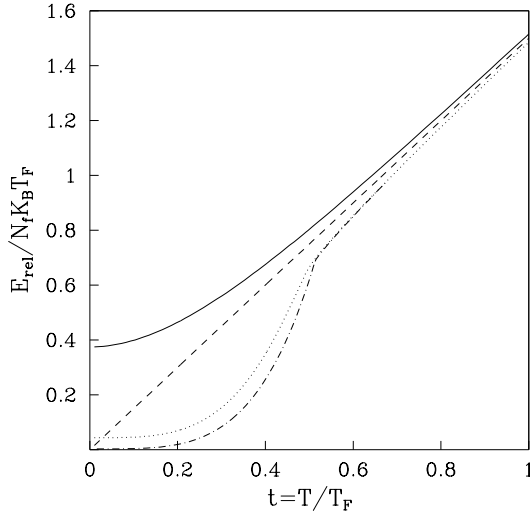


FIG. 1.

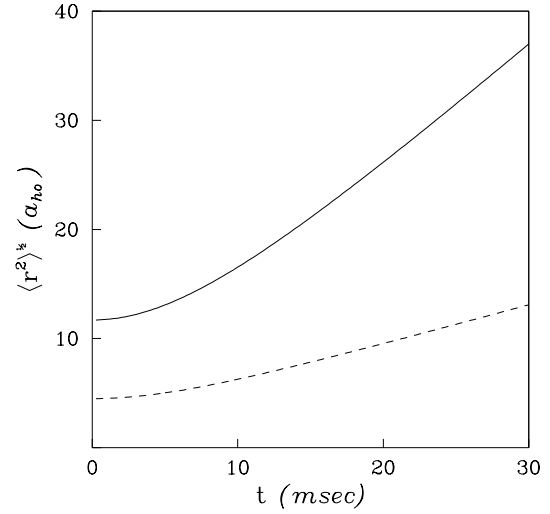


FIG. 2.

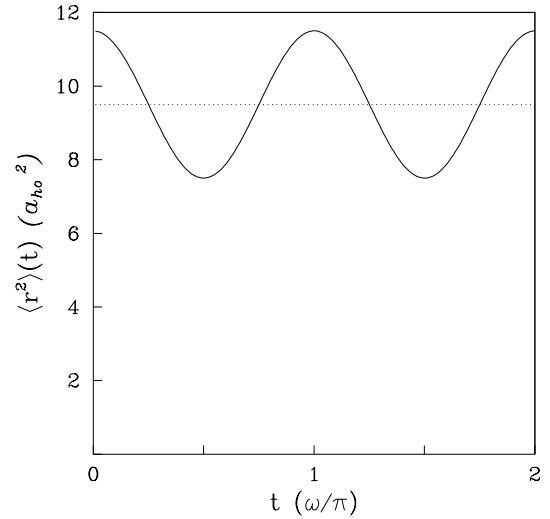


FIG. 3.